arXiv:1601.04002v1 [nucl-ex] 15 Jan 2016

Coulomb breakup of neutron-rich ^{29,30}Na isotopes near the island of inversion

A . Rahaman[1], Ushasi Datta*[1,2], T. Aumann[2,3], S. Beceiro-Novo[4], K. Boretzky[2], C. Caesar[2], B.V. Carlson[5], W.N. Catford[6], S. Chakraborty[1], M. Chartier[7], D. Cortina-Gil[4], G. De. Angelis[8], D. Gonzalez-Diaz[2,9], H. Emling[2], P. Diaz Fernandez[4], L.M. Fraile[10], O. Ershova[2], H. Geissel[2,11], B. Jonson[12], H. Johansson[12], N. Kalantar-Nayestanaki[13], R. Krücken[14], T. Kröll[14], J. Kurcewicz[2], C. Langer[2], T.Le Bleis[14], Y. Leifels[2], G. Münzenberg[2], J. Marganiec[2], T. Nilsson[12], C. Nociforo[2], F. Nowacki[15], A. Najafi[13], V. Panin[2], S. Paschalis[3], R. Plag[2], A. Poves[16], I. Ray[1], R. Reifarth[2], C. Rigollet[13], V. Ricciardi[2], D. Rossi[2], H. Scheit[3], H. Simon[2], C. Scheidenberger[2,11], S. Typel[2], J. Taylor[7], Y. Togano[17], V. Volkov[3], H. Weick[2], A. Wagner[18], F. Wamers[2], M. Weigand[2], J.S. Winfield[2], D. Yakorev[18], and M. Zoric[2]

[1]Saha Institute of Nuclear Physics, Kolkata 700064, India
[2]GSI Helmholtzzentrum fur Schwerionenforschung GmbH, D-64291 Darmstadt, Germany
[3]Technische Universitat Darmstadt, 64289 Darmstadt, Germany
[4]Universidade de Santiago de Compostela, 15706 Santiago de Compostela, Spain
[5]Instituto Tecnologico de Aeronautica, Sao jose dos Campus, Brazil
[6]University of Surrey, Guildford GU2 5XH, United Kingdom
[7]University of Liverpool, Liverpool L69 7ZE, United Kingdom
[8]INFN, Legnaro, Italy
[9]Zaragoza University, 50009 Zaragoza, Spain
[10]Universidad Complutense de Madrid, CEI Moncloa, E-28040 Madrid, Spain
[11]II. Physikalisches Institut, D-35392 Giessen
[12]Fundamental Fysik, Chalmers Tekniska Hogskola, S-412 96 Goteborg, Sweden
[13]KVI-CART, University of Groningen, Groningen, The Netherlands

[14]Physik Department E12, Technische Universität München, 85748 Garching, Germany
[15]IN2P3-CNRS et Univ. Luis Pastour, Stasbourg, France
[16]Universidad Autonoma de Madrid, E-28049 Madrid Spain
[17]The Institute of Physical and Chemical Research (RIKEN), Japan
[18]Helmholtz-Zentrum Dresden-Rossendorf, D-01328 Dresden, Germany

January 18, 2016

Abstract

First results are reported on the ground state configurations of the neutron-rich ^{29,30}Na isotopes, obtained via Coulomb dissociation (CD) measurements as a method of the direct probe. The invariant mass spectra of those nuclei have been obtained through measurement of the four-momentum of all decay products after Coulomb excitation on a ^{208}Pb target at energies of 400-430 MeV/nucleon using FRS-ALADIN-LAND setup at GSI, Darmstadt. Integrated Coulomb-dissociation cross-sections (CD) of 89 (7) mb and 167 (13) mb up to excitation energy of 10 MeV for one neutron removal from ^{29}Na and ^{30}Na respectively, have been extracted. The major part of one neutron removal, CD cross-sections of those nuclei populate core, in its' ground state. A comparison with the direct breakup model, suggests the predominant occupation of the valence neutron in the ground state of ^{29}Na$(3/2^+)$ and ^{30}Na(2^+) is the d orbital with small contribution in the s-orbital which are coupled with ground state of the core. The ground state configurations of these nuclei are as $^{28}\mathrm{Na}_{gs}(1^+) \otimes \nu_{s,d}$ and $^{29}\mathrm{Na}_{gs}(3/2^+) \otimes \nu_{s,d}$, respectively. The ground state spin and parity of these nuclei, obtained from this experiment are in agreement with earlier reported values. The spectroscopic factors for the valence neutron occupying the s and d orbitals for these nuclei in the ground state have been extracted and reported for the first time. A comparison of the experimental findings with the shell model calculation using MCSM suggests a lower limit of around 4.3 MeV of the sd-pf shell gap in ^{30}Na.

Keywords: neutron-rich nuclei, island of inversion, radioactive ion beam, Coulomb breakup, ground state configuration, spectroscopic factor

1 Introduction

The magic numbers [1, 2] of the nuclei are a benchmark of nuclear structure. The underlying shell gap is the characteristic of the mean nuclear field which consists of many ingredients of the nucleon-nucleon interactions. The modification in the shell gaps through

*corresponding:ushasi.dattapramanik@saha.ac.in

the effects such as the tensor component of the NN force become pronounced with large neutron-proton asymmetries in the exotic nuclei far away from stability. These lead to the disappearance of established magic numbers and the appearance of new ones. The first observation of the disappearance of the magic number (N=20) was reported, based on the mass measurements in the neutron rich ^{31,32}Na [3]. The experimental observation of the higher binding energies of these nuclei is a direct consequence of the large deformation [3]. Later large deformation was also reported in the ground state of ^{32}Mg [4]. This large deformation was explained by considering the intruder effects which suggests a clear vanishing of the shell gap between *sd* and *pf* shell around N =20. The N=20 isotones with Z$\sim 10-12$ are considered to belong to the "island of inversion" [5] where the intruder configurations dominate the ground state wave function. Otsuka et al. considered strongly attractive monopole interaction of the tensor force to describe the shell evolution for several nuclei [7].The attractive $T = 0$ monopole interaction between the $\pi d_{5/2}$ and $\nu d_{3/2}$ orbits changes the size of the $N = 20$ effective energy gap as the protons fill the $d_{5/2}$ orbitals.

The availability of radioactive ion beams provides an unique opportunity to study the evolution of the shell structure of the nuclei far away from the β-stability line and many experimental observations on the non magicity behavior of the neutron-rich nuclei around 'classic' magic number have been reported. It is of particular interest to understand the shell evolution for the nuclei where transition from the normal ground state configuration to the intruder dominated ground state configuration occurs. The experimental studies in this direction may provide a stringent test for the validation of various theoretical predictions of the nucleon-nucleon interactions. In other words, to understand change of nucleon-nucleon interaction, with iso-spin quantum number, the key ingredients are experimental information on ground state configuration of these transition nuclei. So far several studies have been performed using different techniques to investigate this region [8, 9, 12, 11, 13, 14, 15]. Though it is established that valence neutron(s) in the ground state of the neutron-rich Na, Mg, Ne isotopes at N = 20, are occupying pf intruder orbitals, but it is not well established for the neighboring nuclei. The ground state configuration of transitional nuclei from normal to "island of inversion" and experimental information for the transitional nuclei are often contradictory to each other. Terry et al. [16] observed *pf* orbital occupation of valence neutron in the ground state of neutron-rich ^{28,30}Ne (N=18, 20) via knockout measurements. However, the situation is different for ^{30}Mg (N=18). Both knockout [17] and Coulomb excitation data [18] are in agreement with *sd*-shell ground state configuration of this nucleus. No detailed ground state configurations of ^{29,30}Na (N=18,19) is available in the literature. The low-energy level structure of the exotic ^{28,29}Na isotopes have been investigated through β-delayed γ spectroscopy [13] and the authors proposed that around $\sim$ 42 % intruder configuration in the ground state of ^{29}Na [8] is necessary to explain experimental data. Several theoretical model calculations and experimental results [8, 9, 12, 13, 14, 19] suggest a significant reduction of the $sd-pf$ shell gap and the ground state of ^{29,30}Na are dominated by intruder states. ^{30}Na has been investigated using Coulomb excitation at the intermediate energies [9] and transition probability $B(E2: 2^+ \rightarrow 3^+) = 147(21)\ e^2\ fm^4$ was reported. The Knockout reaction by Tajes et al. [20] showed that the momentum distributions of both ^{29,30}Na are almost identical (137 MeV/c and 130 MeV/c respectively) although ^{29}Na (S_n = 4.4

MeV) is much deeply bound than ^{30}Na ($S_n = 2.27$ MeV). This unconventional experimental observation encourage for more experimental investigation. An experimental program (GSI:s306) has been initiated to explore the ground state configurations of the neutron-rich nuclei around N $\sim$ 20 via direct probes at GSI, Darmstadt. The Coulomb break up is a direct method to probe the quantum number of the valence nucleon of loosely bound nuclei [21, 22, 23, 24]. In this letter, first results on wave-function decompositions of the ground state of ^{29,30}Na, studied via Coulomb breakup, are being reported.

2 Experiment

The secondary beam containing ^{29,30}Na isotopes along with others were populated by fragmentation of the ^{40}Ar primary beam with energy 540 MeV/nucleon and separated at FRS [25]. The incoming projectiles were identified event-by-event by measuring the magnetic rigidity, time of flight and relative energy loss of the exotic nuclei. The incoming beam-identification plot is shown in Figure 1. The beam intensity of ^{29,30}Na were around $14\%, 5.5\%$ respectively, of total incoming beam.

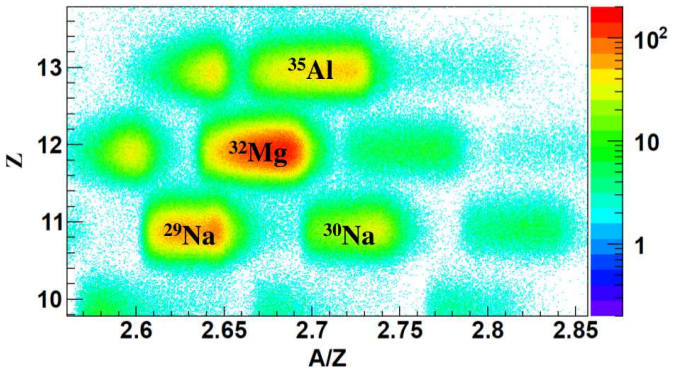

Figure 1: Identification plot for mixed radioactive beam impinging on secondary targets.

The secondary beam (Figure 1) was transported to the experimental site, a neighboring cave C where the complete kinematic measurements were performed using the FRS-ALADIN-LAND setup. The position of the incoming beam before the secondary target and the position of the reaction fragments after the target were accurately measured using double sided Silicon strip detectors (DSSD). The target was surrounded by 162 NaI(Tl) detectors [29], which cover almost 4π solid angle. This detector-array was used for detecting the γ-rays from the excited core of the projectile after the Coulomb breakup. After reaction at the secondary target the reaction fragments as well as the unreacted beam were bent by a Large Dipole Magnet (ALADIN) and ultimately were detected at the time of flight wall detector (TFW) via two scintillator detectors GFI [26, 27]. Out going fragments charge distribution can be obtained through the energy loss at TOF and silicon strip detector (DSSD). Figure 2 shows the charge distribution of out going fragments. The decay product, neutrons were forward focused due to Lorentz boost and detected by the Large Area Neutron Detector (LAND) [28] for the time of flight and position measurements. The reaction fragments were bent at different angles

inside ALADIN depending on their charge to mass ratios. This relative deflection angle was measured using the GFI detectors placed at two different distances at an angle of 15^0 from the original beam direction after the ALADIN. The mass of the outgoing reaction fragments was reconstructed using the deflection angles measured from GFI, the energy loss at TFW, and the time of flight measurement of the reaction fragments. Figure 3 represents the mass of the outgoing fragment against velocity, after one neutron breakup of ^{29}Na. For details of the experimental setup and detector calibration see [30, 31] and references therein.

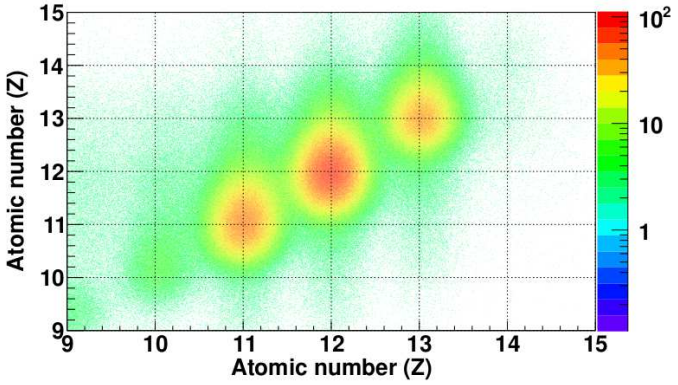

Figure 2: Outgoing fragments charge distribution

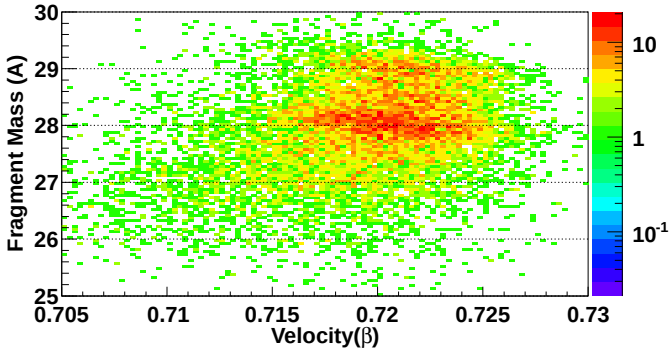

Figure 3: Outgoing fragments mass identification plot after one neutron breakup of ^{29}Na beam on a lead target.

3 Analysis

In this experiment the excitation energy E^* of ^{29,30}Na are determined by measuring four momenta of all the decay products of those nuclei after breakup [21, 22].

$$E^* = \sqrt{\sum m_i^2 + \sum_{i \neq j} \gamma_i \gamma_j m_i m_j (1 - \beta_i \beta_j cos\theta_{ij})} + E_\gamma - m_{proj} \quad (1)$$

In the above equation m_i, m_{proj} are the rest masses of the breakup products and the projectile respectively. β_i, β_j, γ_i, γ_j are the velocities and Lorentz factors of the reaction products respectively. θ_{ij} represents the angle between the reaction products i.e. reaction fragment and the breakup neutron in the present experiment. E_γ is the excitation of the core of the projectile measured with the help of the crystal ball detector.

The excitation energy E^* of ^{29,30}Na were measured using Pb and C targets. The background contributions due to the reactions induced by the materials of the detectors and air column were determined from the data taken without any target and this background data were subsequently subtracted from the data of Pb and C target. Figure 4 (top) shows reaction yields of one neutron breakup against the excitation energy of ^{29}Na using Pb-target (filled circle) and without any target (filled triangle). Similarly, Figure 5 (top) shows the reaction yields of one neutron breakup against ^{30}Na using Pb-target (filled circle) and without any target (filled triangle). The Coulomb dissociation (CD) cross section of those neutron-rich nuclei using the ^{208}Pb target (2.0 g/cm^2) was determined after subtracting the nuclear contribution which was obtained from the data with a ^{12}C target (0.9 g/cm^2) with proper scaling factor [32] (1.8). With change of scaling factor of 10%, the total cross-section of CD would change 1.4%. Filled circle, triangle and square in the lower panel of Figure 4 and Figure 5, respectively show one neutron breakup reaction cross-section of ^{29,30}Na, for Pb-target (Coulomb and nuclear), C-target (nuclear) and pure Coulomb part from Pb target, respectively. The CD cross section for different core excited states can be further differentiated experimentally by the coincidence observation of the characteristic γ-ray of the core fragments with the fragments and neutron [21]. The excitation energy of the excited core state can be obtained from γ-energy sum spectra. The detection efficiencies of the NaI detectors for detecting the γ-rays under the experimental conditions were estimated by GEANT simulations.

The measured invariant mass spectra have been analyzed using the direct breakup model. The neutron-rich nucleus around N = 20, has been considered as a combination of the core and a loosely bound valence neutron which may occupy one or more orbitals e.g. s, d, p etc.. When the projectile passes by a high Z target it may be excited by absorbing the virtual photons from the time dependent Coulomb field [33]. The tail part of the wave-function of the loosely bound neutron is highly sensitive to this virtual photon. Hence due to this interaction the valence neutron moves from bound state to the continuum, while core behaves as a spectator. Thus the nucleus breaks up into a neutron and the core. The electromagnetic breakup of loosely bound nuclei in energetic heavy ion collisions is dominated by dipole excitation due to smaller effective charge for higher multi-polarities [34]. Thus one neutron removal differential Coulomb dissociation cross section (CD) for dipole excitations dσ/dE* decomposes into an incoherent sum of components d$\sigma(I_c^\pi)$/dE* corresponding to different core states (I_c^π), populated after one neutron removal. For each core state, the cross-section further decomposes into incoherent sum over contribution from different angular momenta j of the valence neutron in its initial state. Thus differential cross-section of ^{29,30}Na can be expressed through the following equation [21]:

$$\frac{d\sigma(I_c^\pi)}{dE^*} = \frac{16\pi^3}{9\hbar c} N_{E1}(E^*) \sum_j C^2 S(I_c^\pi, nlj) \times \sum_m | < q|(Ze/A) r Y_m^l |\psi_{nlj}(r) > |^2 \qquad (2)$$

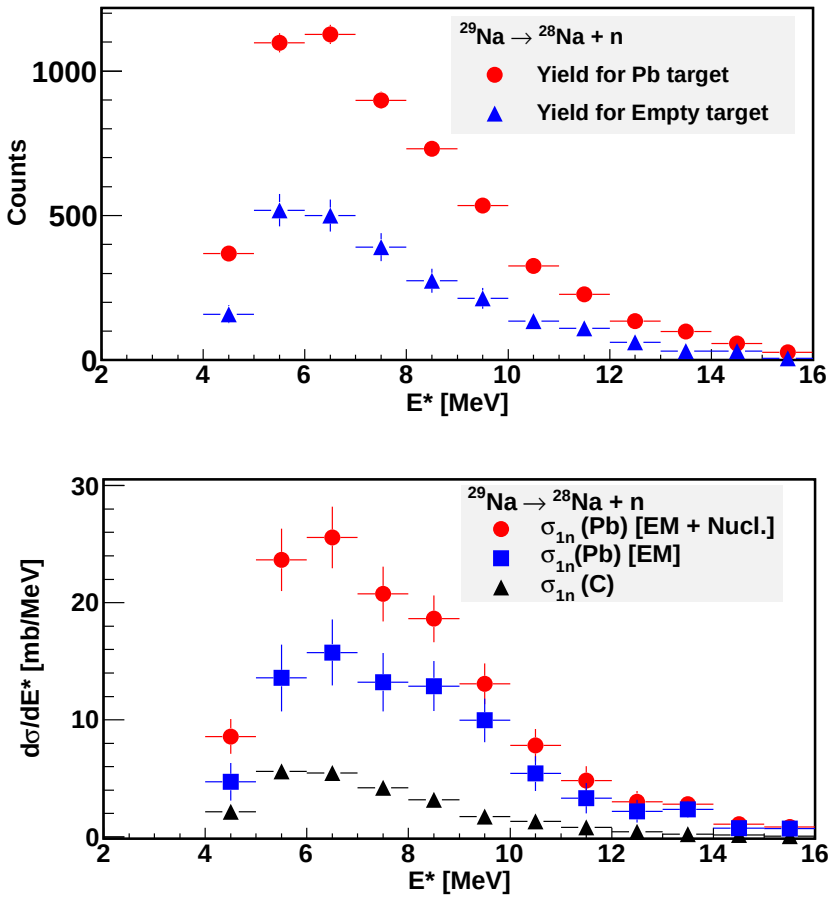

Figure 4: (Top) The yields of one neutron breakup reaction against excitation energy of ^{29}Na using Pb target and without any target have been represented by filled circles and triangles, respectively. (bottom) One neutron breakup cross-sections against excitation energy of ^{29}Na using Pb-target (Coulomb+nuclear), C-target(nuclear) and pure Coulomb of Pb have been denoted by circles, triangles and squares, respectively.

Here, $N_{E1}(E^*)$ is the number of virtual photons as a function of excitation energy E* which can be computed adapting a semi-classical approximation [33]. $\psi_{nlj}(r)$ and $< q|$ represent the single-particle wave function of the valence neutron in the projectile ground state (before breakup) and the final state wave-function of the valence neutron in the continuum (after breakup), respectively. The wave function of the out going neutron in the continuum is considered as a plane wave. $C^2S(I_c^\pi, nlj)$ represents the spectroscopic factor of the valence neutron with respect to a particular core state I_c^π.

Eq. (2) indicates that the dipole strength distribution is very sensitive to the single-particle wave function which in turn depends on the orbital angular momentum and the binding energy of the valence neutron. Thus, by comparing the experimental Coulomb dissociation cross section with the calculated one, information on the ground state properties such as the orbital angular momentum of the valence nucleon and the corresponding spectroscopic factor may be gained. The core state to which the neutron is coupled can

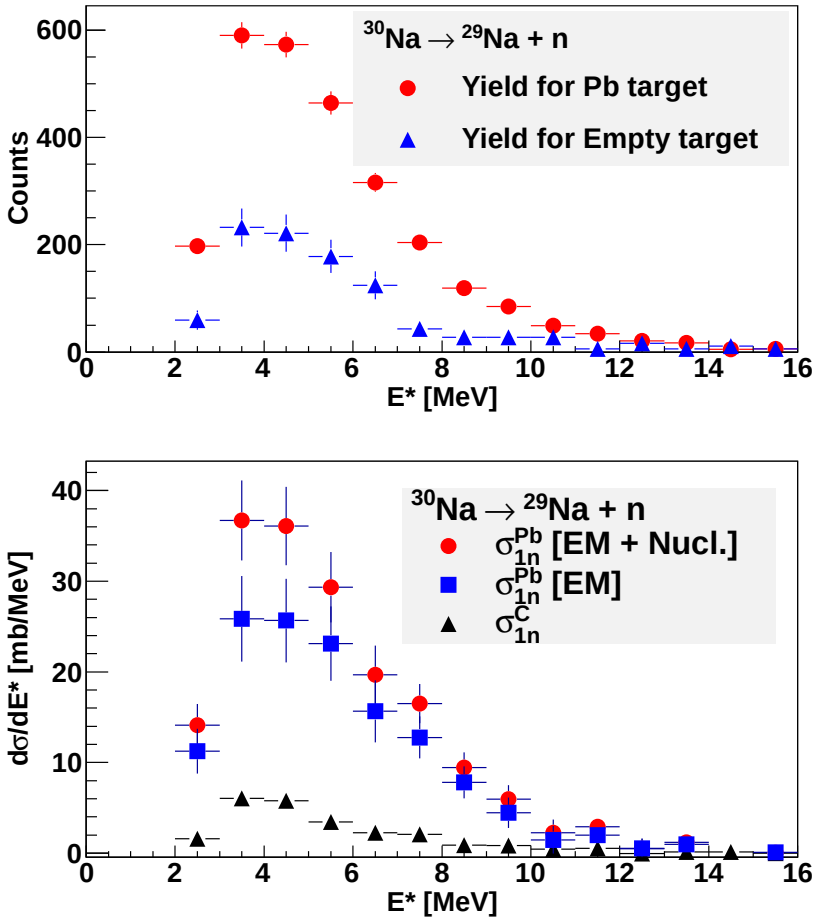

Figure 5: (Top) The yields of one neutron breakup reaction against excitation energy of ^{30}Na for Pb target and without any target have been represented by filled circles and triangles, respectively. (bottom) One neutron breakup cross-sections against excitation energy of ^{30}Na using Pb-target (Coulomb + nuclear), C-target (nuclear) and pure Coulomb part have been denoted by circles, triangles and squares, respectively.

be identified by the characteristic γ -decay of the core after releasing the valence neutron. The Coulomb breakup cross section which leaves the core in its ground state is obtained from the difference between the total cross section and the excited-state(s) contribution(s).

In order to compare the experimental result with the calculated data, one needs to convolute the instrumental response function with the later. The instrumental response for a given value of E^* has Gaussian distribution to a good approximation [35, 36, 37]. The results of all the calculations, shown in this article, are convoluted with the response function.

4 Result

The total Coulomb dissociation cross section for ^{29}Na into ^{28}Na and one neutron amounts to 89 (7) mb, after integration up to 10 MeV excitation energy. No resonance-like structure has been observed. The data analysis for ^{29}Na shows that the major part (72(11) %) of the breakup cross section leaves the core ^{28}Na in its ground state and approximately ($\sim$28(5)%) of the fragments are found in the excited states which could be deduced from the invariant mass spectra, obtained through coincidence of the γ-ray sum spectra with the core fragment (i.e., ^{28}Na) and one neutron. Left panel of the Figure 6 shows the experimental differential Coulomb dissociation cross section with respect to the excitation energy (E^*) of ^{29}Na which breaks up into a neutron and a ^{28}Na fragment in its ground state (filled circles). The spectrum was obtained after subtracting contribution due to the excited states from the total differential cross-section of pure Coulomb breakup of ^{29}Na. The valence neutron of ^{29}Na is sufficiently loosely bound ($S_n = 4.4$ MeV) compared to valence proton ($S_p = 15.9$ MeV). This nucleus can be considered as a core and loosely bound neutron and the calculation for CD cross-section using the direct breakup model [21] have been performed using various valence neutron occupying orbitals. The out going neutron in the continuum is approximated by a plane-wave. To understand the valence neutron occupation orbital with probability, the experimental Coulomb Dissociation cross-section $d\sigma(I_c^\pi)/dE^*$ of ^{29}Na into ground state of ^{28}Na and one neutron have been compared with direct breakup model calculation. All experimental $d\sigma/dE^*$ distributions are shown in figures without acceptance and efficiency corrections for the neutron detector. Instead, the calculated cross sections were convoluted with the detector response obtained from detailed simulations. Comparison between the experimental data on Coulomb dissociation with direct breakup model calculation using p, and combination of s and d orbital, respectively are shown in the figure 6a, 6b, respectively. The experimentally observed shape of the spectrum is in good agreement with the calculated one considering valence neutron in s and d orbital. The solid curve in the figure 6a, 6b represent the calculated $d\sigma(I_c^\pi)/dE^*$ using the direct-breakup model with the valence neutron in the p and combination of s and d orbitals, respectively. The inset of the Figures 6a show the χ^2/N for fitting against the spectroscopic factors of the valence neutron in p. The inset of the Figure 6b, shows three dimensional plot of the χ^2/N for fitting (z-axis in color shade) against the spectroscopic factors of the valence neutron in s, d orbital (x and y axis). It is evident from Figure 6b that the best fit of the experimental data can be obtained

with calculation where the valence neutron is occupying combination of s and d orbitals. The χ^2/N for the fit suggests that the neutron is occupying the s and d orbitals with the spectroscopic factors 0.14 (0.08) and 2.08 (0.3), respectively. The errors quoted in the spectroscopic factors are obtained from The χ^2 distribution and the errors are one sigma i.e, within 68% confidence limit. The dashed and dotted-dashed line in Figure 6b represent the calculated CD cross-section with valence neutron in d and s orbital with above mentioned spectroscopic factors.

The total Coulomb dissociation cross section for ^{30}Na into ^{29}Na and a neutron amounts to 167 (13) mb, after integration up to 10 MeV excitation energy. No resonance-like structure has been observed. The data analysis for ^{30}Na shows that the major part (75 (10)%) of the breakup cross section leaves the core ^{29}Na in its ground state and approximately ($\sim$25 (4)%) of the fragments are found in the excited states. Right panel of figure 6 shows the experimental differential Coulomb dissociation cross section with respect to the excitation energy (E*) of ^{30}Na breaking up into a neutron and a ^{29}Na fragment in its ground state (filled circles). This spectra was obtained after subtracting excited state contribution from the spectra of total differential cross-section of pure Coulomb breakup of ^{30}Na. The valence neutron of ^{30}Na is sufficiently loosely bound (S$_n$ = 2.37 MeV) compared to valence proton (S$_p$ = 17.0 MeV). The experimental Coulomb Dissociation cross-section (dσ/dE*) of ^{30}Na into ground state of ^{29}Na and one neutron have been compared with direct breakup model calculation considering the valence neutron in the p, or combination of s and d orbitals. Inset of the figure shows χ^2/N obtained from fitting with variation of spectroscopic factors. The data can be well reproduced by a fit including contributions from the wave functions involving $l = 0$ and $l = 2$ neutrons, as shown in Figure 6d. The inset of the Figure 6d shows spectroscopic factors of s and d orbital occupation of the valence neutron corresponding to distribution of the χ^2/N. The spectroscopic factors obtained from the fit to the data using the plane-wave approximation for the neutrons occupying the s and d orbitals are 0.08 (0.06) and 2.03 (0.3), respectively. The dashed and dotted-dashed line in Figure 6d represent the calculated CD cross-section using the valence neutron in d and s orbital with respective spectroscopic factors. The ground state spin and parity of ^{30}Na from this experimental results favor $3/2^+\otimes 1/2^+$ i.e. either 2^+ or 1^+.

5 Discussion

The ground state spin and parity of ^{29,30}Na were measured by magnetic resonance [39]. But no detailed measurement on ground state configuration is available. γ-ray spectroscopy data [12, 13, 14, 19] were interpreted as intruder dominated ground state configuration. Present experimental CD cross sections of ^{29,30}Na along with the calculated one from the direct breakup model have been summarized in the table 1. The Coulomb breakup calculation are compared with the experimental findings. The dominant ground state configuration of ^{29}Na is $^{28}\mathrm{Na}_{gs}(1^+) \otimes \nu_{s,d}$. The ground state spin and parity of ^{29}Na from this experiment favor $1^+\otimes 1/2^+$ i.e, either $3/2^+$ or $1/2^+$. A comparison between the spectroscopic factors obtained from this experimental data with shell model calculations using various interaction have been presented in the table 1. In USD-B calculation the

Table 1: Coulomb dissociation cross sections of ^{29,30}Na for various core state and valence-neutron orbitals. Cross sections obtained from the direct-breakup model for neutrons occupying s an d orbitals with a spectroscopic factor of one are given for comparison. The cross sections are integrated up to 10 MeV for ^{29}Na and ^{30}Na. The corresponding spectroscopic factors from shell-model calculations and the ones derived from the experiment are quoted in the last two columns.

Isotope	Core state I^π	Neutron orbital (E; [MeV])	Cross section (mb) Theo.	Expt.	Spectroscopic factor Th-I	Th-II USDB	Expt sdpf-M
^{29}Na	1^+ (0.0)			64(8)			
		$1s$	89			0.16	0.14(0.08)
		$0d$	22		2.18	0.05	2.08(0.3)
	1.0-3.2			25(4)			
^{30}Na	$3/2^+$ (0.0)			125(14)			
		$1s$	205			0.09	0.08(0.06)
		$0d$	56		2.97	0.11	2.03(0.3)
	1.0-3.0			42(6)			

valence space is composed of the *sd* shell for both protons and neutrons. For *sdpf*-M, the valence space is composed of the *sd* shell for protons and allows mixing between *sd* and *pf* shell orbitals for neutrons. The Hamiltonian has been recently introduced [40]. The calculated spectroscopic factors are given in table 1. Both USD-B [38] shell model calculation, and MCSM shell model calculations [8] favor $3/2^+$ as the ground state spin and parity of ^{29}Na. This is in agreement with the earlier experimentally measured value [39]. Utsuno et al., [8] showed that the measured two neutron separation energy, magnetic and electric moments of ^{29}Na can be explained by both USD and *sdpf*-M. The excited core contributions in their ground state configuration are around $\sim$ 28(5)% as per our experimental observation for ^{29}Na isotopes and the core excited state contribution above 2.0 MeV is around 12%. To a simple approximation, if this amount is considered wholly due to $2p-2h$ configurations, then according to MCSM [8] calculations, one can obtain 4.8 MeV as lower limit of the $sd-pf$ shell gap in ^{29}Na. It is clear from Figure 6b that the experimental spectroscopic factor for the valence neutron in the *d* orbital coupled with $^{28}\mathrm{Na}_{gs}(1^+)$ is 2.08 (0.3) and this is in good agreement with USD-B shell model calculation (2.18). Measured mass of ^{29}Na can be explained by sd-shell model calculation [43].

The ground state spin and parity of ^{30}Na has been measured earlier as being 2^+ [39] and this value can be reproduced by both USD [38] shell model and MCSM shell model calculations [8]. No experimental data on ground state configuration of this nucleus is available. To explain measured reduced matrix element of this isotope, it has been considered that the ground state is pure two-particle-two-hole deformed ground state [19]. But present experimental data favors $^{29}Na_{gs}(3/2^+) \otimes \nu_{s,d}$ as major ground state configuration of ^{30}Na (N=19) and the core ^{29}Na excited state contribution i.e, particle hole configurations in the ground state is around 42 (6) mb (25(4)% of total CD cross-section). If it is approximated that the excited states contributions are entirely due to $2p-2h$ configurations then a comparison of our experimental findings with shell-model calculation using the MCSM [8] suggests a lower limit of $sd-pf$ shell gap, around 4.3 MeV in this nucleus. For the first time experimental quantitative spectroscopic factors of valence neutron in the *s* and *d* orbital have been measured. Unlike, ^{29}Na, for ^{30}Na, the experimental spectroscopic factor for occupation of *d*-orbital (2.03) deviates from *sd*-shell (USD-B) calculation (2.97). Hence reduced spectroscopic factor of valence neutron occupying *d*-orbital could be due to particle hole configuration across the reduced sd-pf shell gap. Since ground state spin and parity of this neutron-rich nucleus is 2^+, the valence neutron occupying *pf* orbital, should be coupled with negative parity excited states of ^{29}Na. So far very little is known about the excited states of ^{29}Na. On the other hand, Coulomb breakup cross-section using direct breakup model for valence neutron in $f_{7/2}$ orbital coupled with core excited state of 1.5 MeV is around 21 mb and it further reduced to 10 mb when coupled with 3.0 MeV excited core state. When valence neutron is occupying *p* orbital, the direct breakup model calculation for same situation is 108 mb and 67 mb, respectively. Considering experimental excited state CD cross-section, 42 (6)mb, it may be possible that valence neutron across the shell gap is occupying either pure *f* or *p* orbital or mixing of *p* and *f* orbital.

In a nut-shell, present experimental data of Coulomb breakup suggests that ground state properties of ^{29}Na can be explained by USD-B shell model calculation. But the situation is different for that of ^{30}Na. The spectroscopic factor for valence neutron in *d*

orbital is almost 1/3 reduced compared to USD-B calculation. This could be tentatively, for particle hole configuration across the shell gap and valence neutron may occupy either f or p orbital or mixing of both pf orbital. Thus, it may be concluded that boundary of "island of inversion" has been started from ^{30}Na, instead of ^{29}Na. Wildenthal et al. [43], showed that measured mass of ^{29}Na can be explained by USD shell model calculation but the same for ^{30}Na was not fully reproduced by sd-shell model calculation. The measured B(E2; $2^+ \rightarrow 3^+$) value for ^{30}Na [9, 10] is around 30% lower than the value calculated by MCSM with the $sdpf$-M interaction. However more details theoretical calculation is necessary to understand nucleon-nucleon interaction for this neutron-rich nuclei near "island of inversion".

6 Conclusion

First results on Coulomb breakup measurements of the neutron-rich ^{29,30}Na nuclei, at energies of 400-430 MeV/nucleon has been reported. The observed low-lying dipole strength in these neutron-rich Na isotopes can be understood as a direct-breakup mechanism and no resonance like structure has been observed. The shape of the experimental differential Coulomb dissociation cross section and its comparison with the calculated cross section suggests the predominant ground-state configuration as $^{28}\mathrm{Na}(1^+) \otimes \nu_{s,d}$ and $^{29}\mathrm{Na}(3/2^+) \otimes \nu_{s,d}$ for ^{29}Na and ^{30}Na respectively. The ground state spin and parity of these nuclei, obtained from present measurement are in agreement with earlier reported values. Thus the first results on ground state configurations and qualitative spectroscopic information of valence neutron occupying the s, d orbitals, obtained via direct method have been reported in this letter. According to this experimental results, the valence neutron is occupying mainly d orbital for both the neutron-rich Na nuclei (N=18,19). But experimentally obtained spectroscopic factor (2.08 (0.3 for valence neutron in d orbital of ^{29}Na is in closer agreement with modified sd-shell (USD-B) calculation (2.18). On the other hand the same for ^{30}Na is different and experimentally obtained spectroscopic factor for valence neutron in d orbital is much reduced 2.03 (0.3) compared to sd-shell (USD-B) calculation (2.97). This could be due to particle-hole excitation of the valence neutron across the shell-gap. A comparison of our experimental findings on the core excited states contributions in the ground state configuration with the shell-model calculation using the MCSM suggests a lower limit of the $sd - pf$ shell gap in ^{30}Na of around 4.3 MeV. Thus present experimental data pointed that ^{30}Na is the boundary of "island of inversion", instead of ^{29}Na. However more detail theoretical calculation is necessary to understand the nucleon-nucleon interaction for this neutron-rich nuclei near "island of inversion".

Acknowledgement

We are thankful to the accelerator people of GSI for their active support during the experiment. Authors are thankful to Prof. B.A. Brown, Michigan state University for providing us shell model calculation and Prof. Sudeb Bhattacharya, Kolkata for critically reviewing the manuscript and suggestions. Author, Ushasi Datta acknowledges Alexander von Humboldt foundation, Germany and SEND project grants (PIN:11-R&D-SIN-5.11-

0400) from Department of Atomic Energy (DAE), Govt. of India for financial support for work.

References

[1] M. Geoppert Mayer, Phys. Rev. **75** (1949) 1969

[2] O. Haxel et al., Phys. Rev. **75** (1949) 1766

[3] C. Thibault et al., Phys. Rev. C **12** (1975) 644

[4] T. Motobayashi et., al 1995 Phys. Lett. B **346**(1995) 9

[5] E. K. Warburton et al., Phys. Rev. C **41** (1990)1147

[6] T. Otsuka et al., Phys. Rev. Lett. **87** (2001) 162501

[7] T. Otsuka et al., Phys. Rev. Lett. **104** (2010) 012501

[8] Y. Utsuno et al., Phys. Rev. C **70** (2004) 044307

[9] S. Ettenauer et al., Phys. Rev. C **78** (2008) 017302

[10] B. V. Pritychenko et al., Phys. Rev. C **66** (2002) 024325

[11] H. Mach et al., Eur. Phys. J A **25** (2005) 105

[12] A. M. Hurst et al., Phys. Lett. B **674** (2009) 168

[13] V. Tripathi et al., Phys. Rev. Lett. **94** (2005) 162501

[14] V. Tripathi et al., Phys. Rev. C **76** (2007) 021301(R)

[15] P. Doornenbal et al., Phys. Rev. Lett. **111** (2013) 212502

[16] J. R. Terry et al., Phys. Lett. B **640** (2006) 86

[17] J. R. Terry et al., Phys. Rev. C **77** (2008) 014316

[18] O. Niedermaier et al., Phys. Rev. Lett. **94** (2005) 172501

[19] M. Seidlitz et al., Phys. Rev. C **89** (2014) 024309

[20] C. Rodriguez-Tajes et al., Phys. Rev. C **82** (2010) 024305

[21] U. Datta Pramanik et al., Phys. Lett. B **551** (2003) 63

[22] T. Nakamura et al., Phys. Rev. Lett. **83** (1999) 1112

[23] U. Datta Pramanik et al., Eur. Phys. J. A **25** (2005) 339

[24] U. Datta Pramanik, Prog. in Particle and Nucl. Phys. **59** (2007) 183

[25] H. Geissel et al., Nucl. Instrum. Methods B **70** (1992) 286

[26] J. Cub et al., Nucl. Instrum. Methods A **402** (1998) 67

[27] K. Mahata et al., Nucl. Instrum. Methods A **608** (2009) 331

[28] Th. Blaich et al., Nucl. Instrum. Methods A **314** (1992) 136

[29] V. Metag et al., Nucl. Phys. A **409** (1983) 331

[30] A. Rahaman et al., Eur. Phys. J **66** (2014) 02087

[31] C. Caesar et al., Phys. Rev. C **88** (2013) 034313

[32] C. J. Benesh et al., Phys. Rev. C **40** (1989) 1198

[33] C. A. Bertulani and G. Baur, Physics Reports **163** (1988) 299

[34] S. Typel and G. Baur, Phys. Rev. C **64** (2001) 024601

[35] K. Boretzky et al., Phys. Rev. C **68** (2003) 024317

[36] C. Nociforo et al., Phys. Lett. B **605** (2005) 79

[37] R. Palit R et al., Phys. Rev. C **68** (2003) 034318

[38] B. A. Brown and B. H. Wildenthal, Annu. Rev. Nucl. Part. Sci. **38** (1988) 29

[39] G. Huber et al., Phys. Rev. C **18** (1978) 2342

[40] E. Caurier , F. Nowacki , A. Poves, arXiv:1309.6955

[41] V. Tripathi et al., Phys. Rev. C **73** (2006) 054303

[42] A. T. Reed et al., Phys. Rev. C **60** (1999) 024311

[43] B. H. Wildenthal et al., Phys. Rev. C **22** (1980) 2260

[44] B. A. Brown, Michigan State University private communication

[45] B. A. Brown and W. A. Richter, 2006 Phys. Rev. C **74** (2006) 034315

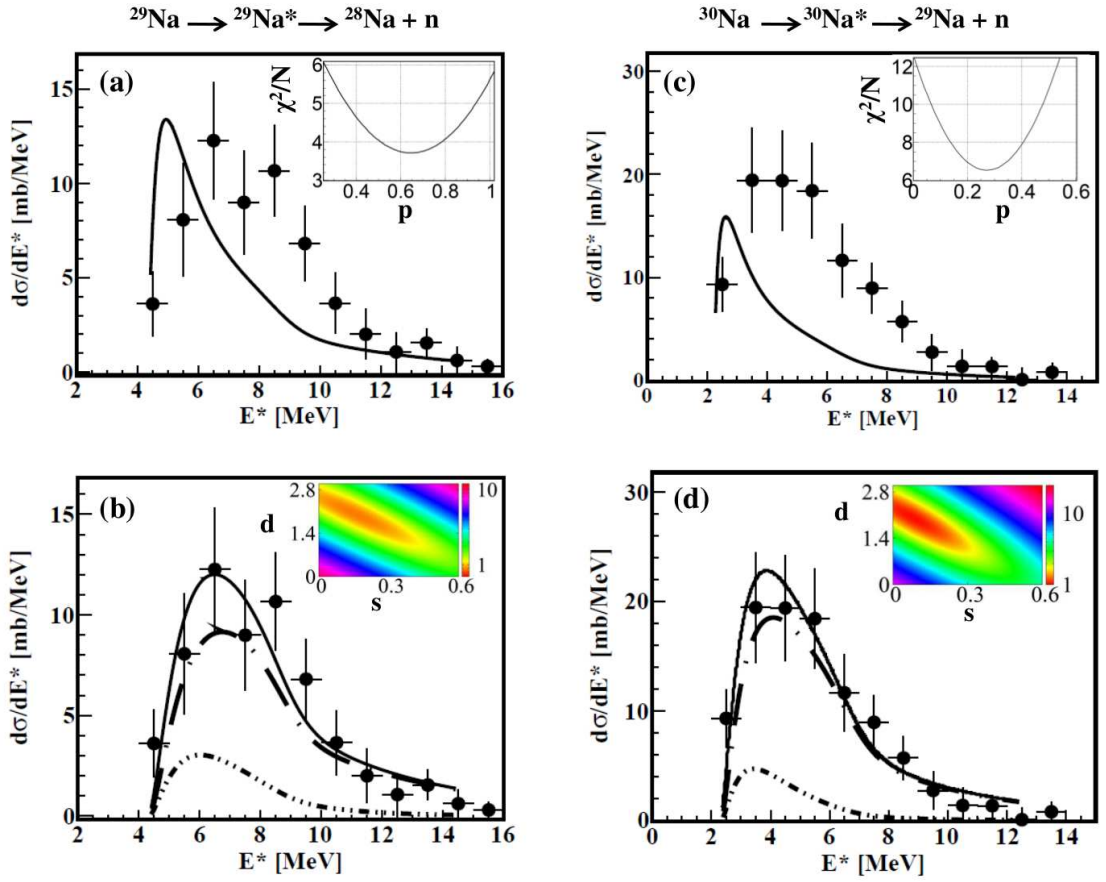

Figure 6: (a-b)Experimental differential pure Coulomb dissociation cross-section of ^{29}Na, breakup into ^{28}Na (gr.) and one neutron. The solid line represents differential CD cross-section using direct breakup model where valence neutron is occupying p-orbital, or combination of s and d-orbital, respectively. The dashed and dotted-dashed line represent the calculated CD cross-section with valence neutron in d and s orbital with respective spectroscopic factors. (c-d) Experimental differential pure Coulomb dissociation cross-section of ^{30}Na against excitation energy and the solid line represents differential CD cross-section using direct breakup model where the valence neutron is occupying p-orbital, or combination of s and d-orbital, respectively. The dashed and dotted-dashed line represent the calculated CD cross-section with d and s wave components. The inset of every figures show the χ^2/N of the fitting between experiment and calculated one against the spectroscopic factor for the valence neutron of that orbital.